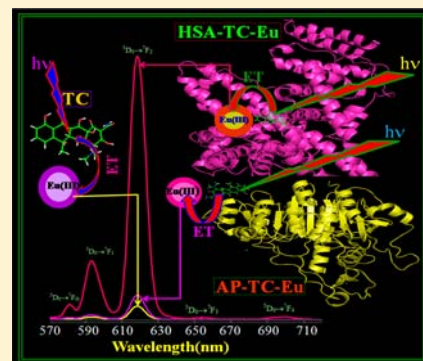


# Tuning of “Antenna Effect” of Eu(III) in Ternary Systems in Aqueous Medium through Binding with Protein

Shyamal Kr Ghorai, Swarna Kamal Samanta, Manini Mukherjee, Pinki Saha Sardar, and Sanjib Ghosh\*

Department of Chemistry and Biochemistry, Presidency University, 86/1, College Street, Kolkata 700073, India

**ABSTRACT:** A simple ternary system containing a protein [human serum albumin (HSA)/bovine serum albumin (BSA)], tetracycline hydrochloride (TC), and Eu(III) in suitable aqueous buffer medium at physiological pH (= 7.2) has been shown to exhibit highly efficient “antenna effect” compared to the binary complex of TC with Eu(III) ( $\text{Eu}_3\text{TC}$ ). The ternary system containing *E. coli* alkaline phosphatase (AP), TC, and Eu(III), however, shows a slight enhancement of Eu(III) emission, although the binding constant of AP with TC is 2 orders of magnitude greater than with BSA/HSA. The enhanced emission of bound TC in the binary systems containing proteins and TC gets quenched in the ternary systems containing HSA/BSA, showing the efficient energy transfer (ET) from TC to Eu(III). Steady state and time-resolved emission studies of each component in all the ternary systems in  $\text{H}_2\text{O}$  and in  $\text{D}_2\text{O}$  medium reveal that Eu(III) is very well protected from the O–H oscillator in the ternary system containing HSA/BSA compared to that containing AP. The docking studies locating the binding site of TC in the proteins suggest that TC binds near the surface of AP. In the case of HSA/BSA, TC resides in the interior of the protein resulting in a large shielding effect of Eu(III). The rotational correlation time ( $\theta_c$ ) determined from the anisotropy decay of bound TC in the complexes and the accessible surface area (ASA) of the ligand in the complexes obtained from the docking studies also support the contention that  $\text{Eu}_3\text{TC}$  is more exposed to solvent in the case of the ternary system consisting of AP, TC, and Eu(III). The calculated radiative lifetime and the sensitization efficiency ratio of Eu(III) in all the systems clearly demonstrate the protein mediated tuning of “antenna effect” in Eu(III).



## 1. INTRODUCTION

The efficient “antenna effect” in Ln(III) complexes in various media is an active area of research for developing LED, silica based fiber optic networks used for telecommunications,<sup>1–3</sup> biological imaging technique, and biomedical assay<sup>4–20</sup> including in vivo detection of cellular functions.<sup>21</sup> The narrow bandwidth of Ln(III) emission in the visible and the NIR region, the longer lifetime, and the large Stokes’ shift from the excitation band are the key features to develop such applications. Time resolved luminescence microscopy as well as two photon microscopy with Ln(III) complexes have also been developed.<sup>22–25</sup>

For these purposes one needs to design organic ligands with suitable architecture which simultaneously enhance the sensitization efficiency and reduce the nonradiative deactivation of the Ln(III) emissive state.<sup>26</sup> Lanthanide-based luminescence hybrid materials have also attracted many researchers.<sup>27</sup> Various hosts studied include sol–gel hybrid, porous hybrid-like zeolites and mesoporous silicates, intercalation compounds, various polymer materials, hydrogels and organic gels, and nanocomposite materials.<sup>27</sup>

The criteria to derive the enhanced “antenna effect” for Ln(III) in the aqueous medium are that (i) the coordinating ligands of Ln(III) must have high absorption  $\pi\pi^*$  singlet state ( $S_1$ ), (ii) the corresponding lowest  $\pi\pi^*$  triplet state ( $T_1$ ) of the ligand acting as donor state must be suitably located compared to the emissive state of Ln(III) in order to minimize the back ET, assuming Dexter’s exchange mechanism is operative in the

sensitization process, (iii) the first coordination sphere of Ln(III) should be protected from the O–H oscillator which is the most effective quencher of the Ln(III) emission through vibronic coupling, and (iv) the complex must be kinetically stable in an aqueous medium. The main challenge in this field, however, is the effective shielding of Ln(III) from the O–H oscillator in the aqueous medium. Since the lowest  $\pi\pi^*$  triplet state acts as a donor state, it is also desirable to increase the intersystem crossing (ISC) rate ( $S_1 \rightarrow T_1$ ), thereby enhancing the population of the ligand triplet state. The presence of a charge transfer (CT) state [arising from metal to ligand or metal to counteranion charge transfer] in between the  $S_1$  and  $T_1$  state of the ligand or between the  $T_1$  state and the emissive state of Ln(III) facilitates a nonradiative path and thus diminishes the efficiency of the sensitization process.

The synthesis of the d–f hybrid complex using Ru(III), Os(III), Ir(III), Re(III), and Pt(III)<sup>28–41</sup> has also gained momentum to enhance the energy transfer (ET) efficiency using the MLCT state as the donor state. The majority of the d–f hybrid complexes, however, exhibit a sensitization effect in nonaqueous medium.

If one compares the “antenna” effect for Tb(III) and Eu(III) in the aqueous medium, the task for enhancement of Eu(III) emission is more difficult since the emissive state  $^5D_0$  or  $^5D_1$  of Eu(III) lies lower in the energy compared to the  $^5D_0$  state of

Received: October 11, 2012

Published: January 15, 2013

Tb(III). Thus, the emissive state of Eu(III) is more susceptible to vibronic coupling with matrix oscillators.

We recently reported efficient synergistic “antenna effect” for Tb(III) in an aqueous medium in a ternary system consisting of a protein (BSA/HSA), a ligand catechin ( $\pm$ ), and Tb(III).<sup>42</sup> We have shown that the catechin complex of Tb(III) gets attached to a particular site of the proteins used in the study. The binding of the Tb(III) complex of catechin with the protein provides an efficient shielding effect of Tb(III) from the O–H oscillator. This shielding effect along with the synergistic energy transfer (ET) from the lowest  $\pi\pi^*$  triplet state of catechin and the triplet state of tryptophan (Trp) residues in proteins were responsible for efficient synergistic ET to Tb(III) in aqueous and D<sub>2</sub>O medium. Furthermore, the triplet state of catechin (24096 cm<sup>-1</sup>) and that of Trp (24224 cm<sup>-1</sup>) are located 3666 cm<sup>-1</sup> and 3794 cm<sup>-1</sup> above the <sup>5</sup>D<sub>4</sub> (20430 cm<sup>-1</sup>) state of Tb(III), respectively. This situation was suitable for synergistic ET as well as minimization of the possibility of back ET from the <sup>5</sup>D<sub>4</sub> state.

This observation prompted us to investigate ternary systems consisting of a protein, simple ligand tetracycline hydrochloride (TC), and Eu(III) in order to develop a very efficient “antenna effect” in Eu(III) in an aqueous medium. The proteins chosen are human serum albumins (HSA), bovine serum albumin (BSA), and alkaline phosphatase from *Escherichia coli* (AP), which are known to bind TC enhancing the TC emission.<sup>43,44</sup> Free TC exhibits emission with a very low quantum yield ( $\phi = 0.26 \times 10^{-3}$ ) at pH 7.2 in an aqueous medium. Since TC is known to bind Eu(III),<sup>45–48</sup> we explored the sensitization effect of Eu(III) in the ternary systems in an aqueous medium with NO<sub>3</sub><sup>-</sup> as the counteranion. A very efficient “antenna effect” is observed in the case of HSA and BSA, whereas in the case of AP, which has a strong binding affinity to TC compared to HSA or BSA, the ET effect is found to be small.

The BSA molecule is made up of three homologous domains which are divided into 9 loops by 17 disulfide bonds. BSA has two tryptophan residues, Trp 134 in the first domain and Trp 213 in the second domain.<sup>49</sup> However, the exact crystal structure of BSA has been unknown until now. HSA, on the other hand, consists of 585 amino acids and is cross-linked by 17 disulfide bonds. HSA contains only a single Trp residue at 214. It has three specific domains, I, II, and III, each of which consists of two subdomains a and b possessing common structural motifs.<sup>50</sup> A comparative study of the amino acid sequences of BSA and HSA by Brown shows that they have similar general structural features, the difference in sequence being generally conservative.<sup>51</sup> Alkaline phosphatase (AP) from *Escherichia coli*, an antibody conjugate, is an important target enzyme in medicinal chemistry.<sup>52–55</sup> Each of the two active sites of the dimeric form of this enzyme contains three metal-binding sites (M1, M2, M3). The M1 and M2 sites are occupied by zinc ions and M3 site is occupied by magnesium ion.<sup>56–62</sup> Each AP monomer contains three tryptophan (Trp) residues at positions 109, 220, and 268.

In this paper we carried out the steady state and time-resolved emission studies monitoring each species in the binary complex (Eu<sub>3</sub>TC) and the ternary systems consisting of BSA/HSA/AP, TC, and Eu(III) to characterize the ET effect in the binary and ternary systems. The ET efficiency observed in the ternary systems has been compared with that observed in the binary system of Eu<sub>3</sub>TC. Time resolved studies of Eu(III) emission in all the binary and the ternary systems in H<sub>2</sub>O and D<sub>2</sub>O are also used to find the number of water coordination in

the inner sphere of Eu(III) in the ternary systems and in the Eu<sub>3</sub>TC system. Molecular docking studies are employed to find the location of TC in the complexes of TC with proteins as well as to calculate the accessible surface area (ASA) of the amino acid residues of BSA/HSA involved in the binding and the ASA of the bound ligand TC. Tuning of the “antenna effect” in the ternary systems has been evaluated using the docking results and the time-resolved anisotropy decay studies of TC bound to proteins. The observed “antenna effect” in the ternary system containing HSA/BSA is found to be greater than that in the Eu<sub>3</sub>TC–H<sub>2</sub>O<sub>2</sub> system<sup>45</sup> and Tb(III) + catechin + protein system.<sup>42</sup>

## 2. EXPERIMENTAL SECTION

**2.1. Materials and Methods.** All chemicals were of reagent grade, which were used without further purification unless otherwise mentioned. The tetracycline hydrochloride (TC), europium nitrate (Eu(NO<sub>3</sub>)<sub>3</sub>), serum albumin from bovine (BSA), serum albumin from human (HSA), alkaline phosphatase from *Escherichia coli* (AP), and  $\alpha,\alpha,\alpha$ -Tris-(hydroxymethyl)-methylamine were purchased from Sigma–Aldrich, USA. The 0.1 M Tris-HCl buffers of pH 7.2 and pH 8.0 were prepared in triply distilled water and used for making all experimental solutions. The binary complexes of TC and Eu(III) were prepared by mixing of 3:1 mol ratio of Eu(NO<sub>3</sub>)<sub>3</sub>:TC. The particular composition used is discussed in section 3.3. The ternary systems were prepared by using 75  $\mu$ M Eu(III), 25  $\mu$ M TC, and 25  $\mu$ M BSA/HSA in the buffer of pH 7.2 and 15  $\mu$ M Eu(III), 5  $\mu$ M TC, and 5  $\mu$ M AP in the buffer of pH 8.0. The temperature during all experiments was maintained at 25  $\pm$  0.1  $^{\circ}$ C, unless otherwise mentioned.

**2.2. Instrumentation.** UV–vis absorption spectra were recorded on a Hitachi U-4010 spectrophotometer at 298 K. The steady state emission measurements were carried out using a Hitachi Model F-7000 spectrofluorimeter equipped with a 150-W xenon lamp at 298 K using a stoppered cell of 1 and 0.5 cm path length for the measurement in pH 7.2 and pH 8.0, respectively.

The lifetime of the singlet state was measured by using TCSPC from PTI, USA, using the subnanosecond pulsed LED source (280 and 370 nm having a pulse width of 600 ps [full width at half-maximum] (from PicoQuant, Germany) operating at a high repetition rate of 10 MHz driven by a PDL 800-B driver, PicoQuant, Germany. LED profiles were measured at the respective excitation of 280 or 370 nm with a band pass of 3 nm using Ludox as the scatterer. Decay measurements using “magic angle” detection with an emission polarizer set at 54.7 $^{\circ}$  were carried out, and no detectable difference in the fitted  $\tau$  values with those obtained from normal decay measurements were observed. Fluorescence quantum yield ( $\phi_D$ ) was determined in each case by comparing the corrected emission spectrum of the samples with that of quinine sulfate in 0.1 N H<sub>2</sub>SO<sub>4</sub> ( $\phi_D = 0.54$ ).<sup>63</sup>

The decay parameters were recovered using a nonlinear iterative fitting procedure based on the Marquardt algorithm.<sup>64</sup> The deconvolution technique used can determine the lifetime up to 150–200 ps. The quality of the fit has been assessed over the entire decay, including the rising edge, and tested with a plot of weighted residuals and other statistical parameters, for example, the reduced  $\chi^2$  ratio.<sup>65</sup>

The transients of the Eu(III) emission in the complexes in the microsecond region were also acquired by phosphorescence decay mode in QM-30 fluorimeter from PTI, USA, using a gated detection system having start and end window times of 0 and 6000  $\mu$ s, respectively. The decay times in the milliseconds or longer range were measured by the phosphorescence time based acquisition mode of the QM-30 fluorimeter in which emission intensity is measured as a function of time. The rise times and decay parameters were recovered using a nonlinear iterative fitting procedure based on the Marquardt algorithm.<sup>64</sup> The mean lifetimes,  $\langle\tau\rangle$ , for biexponential decays were calculated using the equation

$$\langle \tau \rangle = (\alpha_1 \tau_1 + \alpha_2 \tau_2) / (\alpha_1 + \alpha_2) \quad (1)$$

**2.3. Anisotropy Measurement.** Anisotropy decay measurement was also carried out in a Time Master Fluorimeter (PTI, USA) using PLS-370 with a pulse width  $\sim 600$  ps [full width at half-maximum] (from PicoQuant, Germany) and motorized Glen Thompson polarizer. The anisotropy,  $r(t)$  is defined as

$$r(t) = [I_{VV}(t) - G \times I_{VH}(t)] / [I_{VV}(t) + 2G \times I_{VH}(t)] \quad (2)$$

where  $I(t)$  terms are defined as intensity decay of emission of TC with excitation polarizer orientated vertically and the emission polarizer orientated vertically and horizontally, respectively:

$$G = I_{HV}(t) / I_{HH}(t) \quad (3)$$

where  $G$  is the correction term for the relative throughput of each polarization through the emission optics. The entire data analysis was done with the software Felix 32 which analyzes the raw data  $I_{VV}$  and  $I_{VH}$  simultaneously by a global multiexponential program and then the deconvolved curves ( $ID_{VV}$  and  $ID_{VH}$ ) are used to construct  $r(t)$ <sup>65</sup>; from the fitted curve the correlation time ( $\theta_c$ ) can be recovered.

**2.4. Docking Studies.** The crystal structures of HSA (PDB entry IAO6) and alkaline phosphatase (PDB ID: 3BDG) are obtained from the Protein Data Bank.<sup>66</sup> Since the structure of bovine serum albumin (BSA) is unavailable in the PDB, a homology model was used for the docking studies.<sup>67–71</sup> The three-dimensional structure of the tetracycline was obtained by Sybyl 6.92 (Tripos Inc., St. Louis, USA), and the energy-minimized structure was achieved using Tripos force field and Gasteiger-Hückel charges with a gradient of 0.005 kcal/mol. Details of docking studies and the calculation of accessible surface area (ASA) in the free protein and the complex have been described in detail in our earlier work.<sup>43,44</sup> PyMol was used to visualize the docked conformation and to measure the distances between the ligand and the protein.<sup>72</sup>

The change in accessible surface area for residue  $i$  is calculated using the following equation

$$\Delta ASA^i = ASA_{FreeProtein}^i - ASA_{Protein-TCcomplex}^i \quad (4)$$

If a residue loses more than  $5 \text{ \AA}^2$  ASA on going from the uncomplexed to the complexed state, then it is considered to be involved in the interaction.

### 3. RESULTS

#### 3.1. Absorption Spectra in Aqueous Buffer at 298 K.

The absorption spectra of various species with HSA and BSA are recorded at 298 K in tris buffer of pH 7.2. In the systems containing AP, the pH of the medium is kept at 8.0 (Figure 1).<sup>70</sup> The absorption spectra of free BSA and the binary

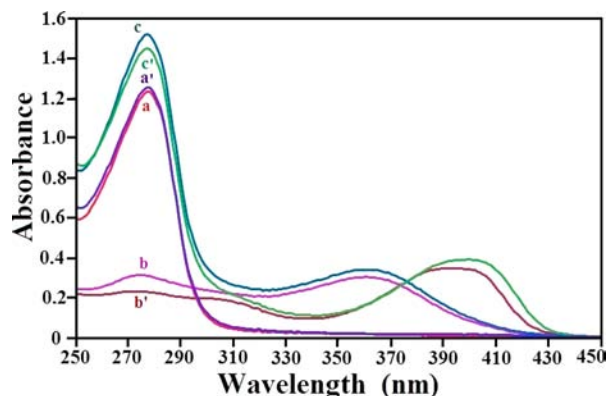


**Figure 1.** Absorption spectra of (a) BSA, (a') BSA + Eu(III), (b) TC, (b') TC + Eu(III), (c) BSA + TC, and (c') BSA + TC + Eu(III) in aqueous buffer at 298 K. [BSA] = 25  $\mu\text{M}$ , [TC] = 25  $\mu\text{M}$ , [Eu(III)] = 75  $\mu\text{M}$ .

complex of BSA with Eu(III) are shown in Figure 1 as a and a', respectively. The counteranion used is  $\text{NO}_3^-$  in all the cases. In Figure 1, b and b' represent the absorption spectra of free TC and the binary complex of TC and Eu(III). The absorption spectra of the binary complex of BSA with TC and the ternary system of BSA and Eu(III) with TC are shown in Figure 1 (c and c', respectively). The TC shows the absorption maximum at 274 and 360 nm. For the complex of TC with Eu(III), the band near 360 nm in the free TC is red-shifted to 395 nm.<sup>45,46</sup> TC has several proton-donating groups which offer different possibilities of complexation with lanthanide ions. The lanthanide (III) ions are reported to coordinate in a bidentate manner to two carbonyl groups of the A ring of tetracycline at low pH ( $\approx 2$ ).<sup>47</sup> It was examined that, upon increase of pH, coordination of tetracycline to lanthanide (III) ions changes from the A ring to the B, C, and D rings and most likely occurs via coordination to the carbonyl group of the C ring and to the OH group of the B ring and/or the D ring.<sup>48</sup> The structure of the  $\text{Eu}_3\text{TC}$  complex has not been determined yet. Although TC offers multiple coordination sites for the binding of Eu(III), the limited amount of TC ligand used suggests that most of the coordination sites of Eu(III) are being occupied by  $\text{H}_2\text{O}$  molecules. The complex of TC with BSA shows the bands at 277 and 360 nm. The absorbance at 277 nm is found to be the sum of the individual absorbances of TC and BSA. The absorption band near 360 nm is shifted to the red region at 395 nm in the ternary system (BSA and Eu(III) with TC) as compared to the binary complex of TC with BSA. The absorbance pattern is also found to be similar for the binary and the ternary systems prepared using HSA and AP.

#### 3.2. Steady State and Time Resolved Emission Studies in Aqueous Buffer at 298 K.

**3.2.1. Using Excitation of TC.** The emission spectra of TC in the free state, in the binary complexes [BSA with TC and TC with Eu(III)], and in the ternary system of BSA and Eu(III) with TC are shown in Figure 2A with  $\lambda_{\text{exc}} = 395$  nm. The emission intensity of TC is enhanced with the addition of BSA, and the  $\lambda_{\text{max}}$  is blue-shifted from 510 to 498 nm. The intensity of TC emission is largely quenched (Table 1) in the binary complex of TC with Eu(III) compared to free TC. In the ternary system of BSA and Eu(III) with TC, the emission of TC gets almost completely quenched compared to that in the binary complex of BSA and TC. The quenching is accompanied by concomitant enhancement of the Eu(III) emission ( $^5\text{D}_0 \rightarrow ^7\text{F}_0$  at 581 nm,  $^5\text{D}_0 \rightarrow ^7\text{F}_1$  at 594 nm,  $^5\text{D}_0 \rightarrow ^7\text{F}_2$  at 618 nm,  $^5\text{D}_0 \rightarrow ^7\text{F}_3$  at 650 nm,  $^5\text{D}_0 \rightarrow ^7\text{F}_4$  at 700 nm) as compared to that of free Eu(III) in the same buffer under similar experimental conditions (Figure 2A).

The  $\lambda_{\text{max}}$  of the TC emission in the binary complex of TC with HSA is blue-shifted from 510 to 489 nm. However, the  $\lambda_{\text{max}}$  in the binary complex of TC with AP remains the same as that of free TC emission. Otherwise, the similar trend of TC emission in all the binary complexes and ternary systems is observed for HSA and AP (Figure 2B,C). The quantum yield of TC emission in all the binary and ternary complexes is given in Table 2. The enhancement of Eu(III) emission is about 20 times in the systems containing HSA or BSA, whereas the enhancement is only about 2 times in the systems containing AP compared to that of the binary complex of  $\text{Eu}_3\text{TC}$ .

The decay of TC emission in the free state and in the complex with BSA is measured in tris-HCl buffer of pH 7.2 monitored at 510 nm with  $\lambda_{\text{exc}} 370$  nm (Figure 3A). The enhancement of the lifetime of the TC emission is observed in the binary complex of TC with BSA compared to that of free

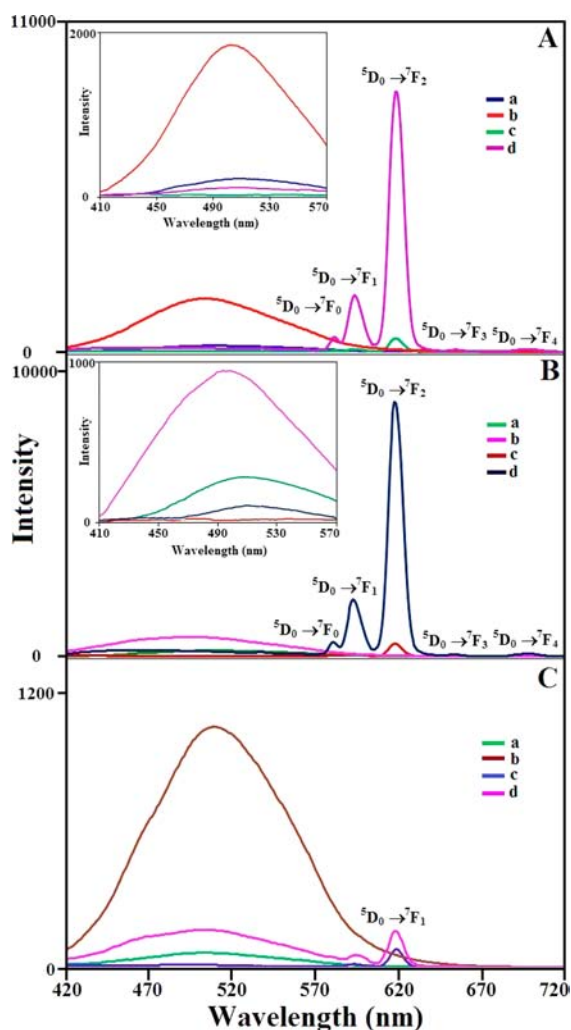


**Figure 2.** (A) Emission spectra of (a) TC, (b) BSA + TC, (c) TC + Eu(III), and (d) BSA + TC + Eu(III) in aqueous Tris-HCl buffer of pH 7.2; [BSA] = 25  $\mu\text{M}$ , [TC] = 25  $\mu\text{M}$ , [Eu(III)] = 75  $\mu\text{M}$ . (B) Emission spectra of (a) TC, (b) HSA + TC, (c) TC + Eu(III), and (d) HSA + TC + Eu(III) in aqueous Tris-HCl buffer of pH 7.2; [HSA] = 25  $\mu\text{M}$ , [TC] = 25  $\mu\text{M}$ , [Eu(III)] = 75  $\mu\text{M}$ . (C) Emission spectra of (a) TC, (b) AP + TC, (c) TC + Eu(III), and (d) AP + TC + Eu(III) in aqueous Tris-HCl buffer of pH 8.0; [AP] = 5  $\mu\text{M}$ , [TC] = 5  $\mu\text{M}$ , [Eu(III)] = 15  $\mu\text{M}$  at 298 K;  $\lambda_{\text{exc}}$  = 395 nm, excitation band pass = 10 nm and emission band pass = 5 nm in each case.

TC (Table 2). The decay fits nicely with two-component analysis (Table 2). The same decay trend is observed for the complex with HSA and AP (Table 2). It is to be noted that the decay of TC emission in the binary complex of TC with Eu(III) and in the ternary systems of BSA/HSA [BSA, Eu(III) with TC and HSA, Eu(III) with TC] could not be measured due to very low intensity. However, the decay of TC emission has been measured in the ternary system of AP, Eu(III) with TC, since the quenching of TC emission is observed to be much less (Table 2).

**3.2.2. Using Excitation of Proteins.** We also carried out the emission studies using excitation of proteins in all the systems. The emission spectra of free BSA, the binary complexes of BSA with Eu(III) and BSA with TC, and the ternary system of BSA and Eu(III) with TC are shown in Figure 4A with  $\lambda_{\text{exc}}$  = 280 nm. The emission spectrum of BSA is slightly quenched with addition of Eu(III). The emission intensity of BSA is

considerably decreased in the binary complex of BSA with TC. However, the emission is not further quenched upon addition of Eu(III) in this system. The  $\lambda_{\text{max}}$  of the emission of BSA in the different systems remains the same at 340 nm, confirming that BSA retains its tertiary structure. The lifetime of Trp emission of BSA is also found to remain the same in the free protein and in the complex with Eu(III) (Figure 4B, Table 3). But the lifetime of Trp emission of BSA is only slightly decreased in the binary complex of BSA with TC and the ternary system of BSA and Eu(III) with TC (Table 3). In the free protein and the complexes of the proteins, the decay of Trp emission is found to fit with two components. The value of average lifetime ( $\langle\tau\rangle$ ) for free protein match very well with the reported data.<sup>73,74</sup> The same trend of emission spectra and lifetime of the Trp emission is observed for the complexes with HSA and AP (Table 3).

It is to be noted that in the binary system of protein and Eu(III), the intensity of the emission from Eu(III) remains the same as that in the free  $\text{Eu}(\text{NO}_3)_3$  in aqueous medium at the same pH, suggesting that Trp residues of proteins are not taking part in the ET process. It is further observed that the enhancement of Eu(III) emission in all the ternary systems with  $\lambda_{\text{exc}}$  = 280 nm is much less as compared to that observed with  $\lambda_{\text{exc}}$  = 395 nm.

**3.3. Binding Constant of Tetracycline and Eu(III).** In order to determine the composition of the complex of TC and Eu(III) in tris-HCl buffer, we followed the enhancement of Eu(III) emission due to the addition of different concentrations of TC (Figure 5A). It was observed that a 3:1 ratio of metal–ligand composition gives a saturation of the luminescence intensity of Eu(III) ( $^5\text{D}_4 \rightarrow ^7\text{F}_5$  peak) (Figure 5C), confirming the composition  $\text{Eu}_3\text{TC}$  of the complex. The binding interaction between TC and Eu(III) was examined by determining the binding constant from the luminescence intensity of the  $^5\text{D}_0 \rightarrow ^7\text{F}_2$  peak of Eu(III) as a function of added TC concentration employing the modified Benesi-Hilderbrand equation<sup>75–77</sup>

$$[F_\infty - F_0]/[F_x - F_0] = 1 + 1/K[Q] \quad (5)$$

where  $F_0$ ,  $F_x$ , and  $F_\infty$  are the luminescence intensity of Eu(III) in the absence of TC, at an intermediate TC concentration, and at a concentration of complete interaction, respectively;  $K$  being the binding constant and  $[Q]$  the concentration of added TC.

The slope of the linear plot of  $[F_\infty - F_0]/[F_x - F_0]$  against the  $[Q]^{-1}$  provides the binding constant ( $K$ ). Such a plot of the complex of TC with Eu(III) is shown in Figure 5B. The calculated binding constant ( $K$ ) is  $9.46 \times 10^4 \text{ M}^{-1}$  (Table 2).

**3.4. Enhancement Factor and Lifetime of Eu(III) in Various Systems at 298 K.** The emission of the Eu(III) ion is greatly enhanced in the ternary system of BSA/HSA and Eu(III) with TC compared to that in the binary complex of TC with Eu(III) (Figure 2A,B). The enhanced intensity ratio of the band ( $^5\text{D}_0 \rightarrow ^7\text{F}_1$ ) at 593 nm and ( $^5\text{D}_0 \rightarrow ^7\text{F}_2$ ) at 618 nm of Eu(III) in different binary and ternary complexes compared to that of free  $\text{Eu}(\text{NO}_3)_3$  is shown in Table 1. The enhancement in the ternary systems could be due to shielding of Eu(III) environments from the potential quencher, namely, the OH-oscillator or efficient intramolecular energy transfer from TC to Eu(III) or both. The enhancement of the luminescence emission of Eu(III) ion in the ternary system of AP and TC with Eu(III) is not very significant as compared to the ternary system of HSA or BSA (Figure 2C, Table 1). It is to be noted

**Table 1. Quenching of Emission of the TC and Enhancement of Luminescence Emission of Eu(III) Ion in the Binary Complex and Ternary Systems in Aqueous Tris-Buffer at 298 K<sup>a</sup>**

medium	system	quenching of the fluorescence band ( $S_1 \rightarrow S_0$ ) ( $I_F/I_F^0$ ) <sup>b</sup> of TC emission ( $\lambda_{exc} = 395$ nm)	enhancement of Eu(III) emission at 593 nm ( $^5D_0 \rightarrow ^7F_1$ ) transition ( $I_M/I_M^0$ ) <sup>c</sup> ( $\lambda_{exc} = 395$ nm)	enhancement of Eu(III) emission at 618 nm ( $^5D_0 \rightarrow ^7F_2$ ) transition ( $I_M/I_M^0$ ) <sup>d</sup> ( $\lambda_{exc} = 395$ nm)
aqueous buffer of pH 7.2	TC + Eu(III)	0.18	43	34
	BSA + TC + Eu(III)	0.08	1021	693
	HSA + TC + Eu(III)	0.09	1074	707
aqueous buffer of pH 8.0	TC + Eu(III)	0.21	42	33
	AP + TC + Eu(III)	0.17	74	65

<sup>a</sup>The intensities are calculated in each case using the total area under the respective band. Error in the measurement of area under the Tb(III) emission =  $\pm 2\%$ . <sup>b</sup> $I_F$  and  $I_F^0$  are the intensities of total fluorescence spectra of the TC in the complex in the presence and in the absence of Eu(III), respectively. <sup>c</sup> $I_M$  and  $I_M^0$  are the intensities of emission for the  $^5D_0 \rightarrow ^7F_1$  transitions of the Eu(III) ion at 593 nm in the complex and in the pure  $\text{Eu}(\text{NO}_3)_3$ , respectively. <sup>d</sup> $I_M$  and  $I_M^0$  are the intensities of emission for the  $^5D_0 \rightarrow ^7F_2$  transitions of the Eu(III) ion at 618 nm in the complex and in the pure  $\text{Eu}(\text{NO}_3)_3$ , respectively.

**Table 2. Singlet State Lifetime ( $\tau$ ), Quantum Yield ( $\phi$ ), Rotational Correlation Time ( $\theta_C$ ), Binding Constant (K), and Accessible Surface Area (ASA) of TC and Proteins in Different Systems at 298 K**

medium	system	lifetime of the Singlet State of TC ( $\lambda_{exc} = 395$ nm)				$\phi_{TC} \times 10^3$	ASA of TC	total $\Delta$ ASA of different residues involved in the proteins (loss of ASA)	$\theta_C$ (ns) $\lambda_{exc} = 370$ nm	binding constant (K) at 298 K
		$\tau_1$ (ns)	$\tau_2$ (ns)	$\langle \tau \rangle$ (ns)	$\chi^2$					
aqueous buffer of pH 7.2	free TC	1.60 (5%)	0.3 (95%)	0.38	1.01	0.26				
	TC + Eu(III)					0.01				$9.5 \times 10^4 \text{ M}^{-1}$
	BSA + TC	2.62 (23%)	1.11 (77%)	1.46	0.99	1.74	264	214	5.0	$4.7 \times 10^4 \text{ M}^{-1}$
	BSA + TC + Eu(III)					0.04				
	HSA + TC	3.22 (11%)	0.96 (89%)	1.21	0.98	0.93	150	302	6.0	$3.1 \times 10^4 \text{ M}^{-1}$
aqueous buffer of pH 8.0	HSA + TC + Eu(III)					0.02				
	free TC	1.73 (1%)	0.36 (99%)	0.37	1.03	0.39				
	AP + TC	2.79 (10%)	0.39 (90%)	0.63	1.10	3.51	382	167	3.6	$6.8 \times 10^6 \text{ M}^{-1}$
	AP + TC + Eu(III)	2.31 (1%)	0.46 (99%)	0.48	0.97	0.48				

that the enhancement in the case of the ternary system containing HSA/BSA is found to be greater than that found in the case of the  $\text{EuTC}-\text{H}_2\text{O}_2$  system.<sup>78</sup>

The transients of acceptor Eu(III) ( $[\text{Eu(III)}] = 75 \mu\text{M}$ ) emission monitoring the band at 618 nm in the binary complex of TC with Eu(III) and in the different ternary systems [BSA, Eu(III) with TC; HSA, Eu(III) with TC and AP, Eu(III) with TC] in aqueous buffer have been measured (Figure 3B) using  $\lambda_{exc} = 395$  nm. All the transients display a rise time followed by acceptor decay. The rise time observed in the binary and the ternary systems containing HSA/BSA are found to be  $4.2 \mu\text{s}$  and  $\sim 7 \mu\text{s}$ , respectively (Table 4). In the case of AP the rise time has been observed to be  $4.6 \mu\text{s}$  (Table 4). The significant change in lifetime of Eu(III) in different complexes with BSA, HSA and AP is shown in Table 4. The enhancement of the emission in the ternary systems compared to the  $\text{Eu}_3\text{TC}$  complex is reflected in the decay of the Eu(III) ion.

**3.5. Emission of Eu(III) in Different Complexes in D<sub>2</sub>O Buffer at 298 K.** The emission of Eu(III) in different binary and ternary systems (TC with Eu(III); BSA, Eu(III) with TC;

HSA, Eu(III) with TC; AP, Eu(III) with TC) has been measured in  $\text{D}_2\text{O}$  buffer with  $\lambda_{exc} = 395$  nm. It was observed that the intensity of luminescence of different peaks and luminescence lifetimes of Eu(III) in  $\text{D}_2\text{O}$  buffer are enhanced compared to that in the different binary and ternary complexes in aqueous buffer (Figures 3B (Inset) and 6). The luminescence lifetime of the  $^5D_0 \rightarrow ^7F_2$  transition at 618 nm is also enhanced as given in Table 4. The rise times of the Eu(III) emission remain practically the same in  $\text{D}_2\text{O}$  medium (Table 4).

**3.6. Docking Studies of the Complexes of TC with Proteins.** Although the binding constant of TC with AP is 2 orders of magnitude greater than that with HSA/BSA,<sup>43,44</sup> the enhancement of the Eu(III) emission is not significant in the ternary system containing AP. It is also noted that the enhanced emission of TC in the TC-HSA or TC-BSA is almost completely quenched in the ternary systems. However, the quenching of TC emission in the ternary system containing AP is much less, implying significantly less ET from TC to Eu(III) (Table 1). To understand this difference we carried out docking

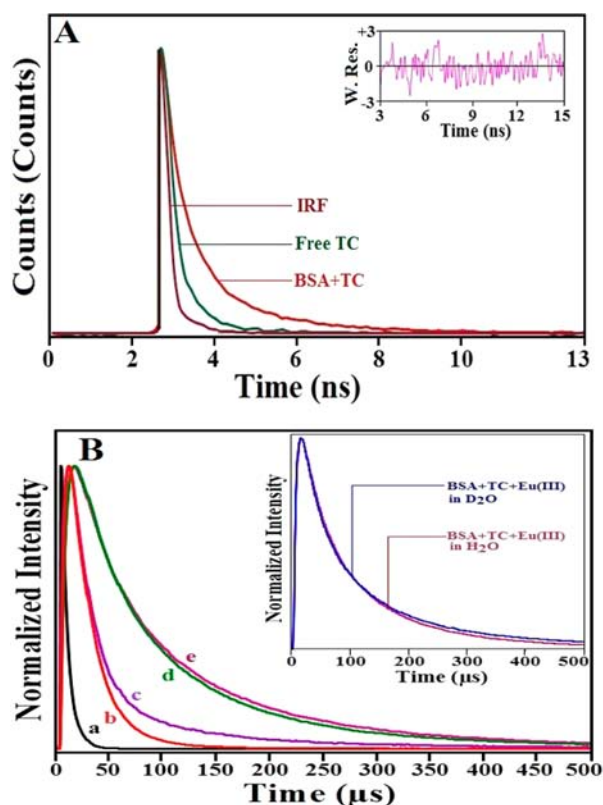


**Figure 3.** (A) Fluorescence decay of TC in the pure state and in the complex with BSA at 298 K in aqueous buffer;  $\lambda_{\text{exc}} = 370$  nm,  $\lambda_{\text{monitor}} = 500$  nm (excitation band pass = 10 nm, emission band pass = 5 nm); [TC] = 25  $\mu\text{M}$ , [BSA] = 25  $\mu\text{M}$ . (B) Transients of Eu(III) (a) IRF, (b) TC + Eu(III), (c) AP + TC + Eu(III), (d) HSA + TC + Eu(III), and (e) BSA + TC + Eu(III) monitored at 618 nm in Tris-HCl buffer at 298 K in different systems. [Inset: Transients of Eu(III) in the ternary system of BSA, Eu(III) with TC in aqueous buffer and in D<sub>2</sub>O buffer];  $\lambda_{\text{exc}} = 395$  nm, excitation band pass = 10 nm, emission band pass = 10 nm. ([BSA] = 25  $\mu\text{M}$ , [HSA] = 25  $\mu\text{M}$ , [TC] = 25  $\mu\text{M}$ , [Eu(III)] = 75  $\mu\text{M}$  at pH = 7.2 and [AP] = 5  $\mu\text{M}$ , [TC] = 5  $\mu\text{M}$ , [Eu(III)] = 15  $\mu\text{M}$ ) at pH = 8.0).

studies of TC with all three proteins to find the location of TC binding. The docked pose of TC in all the ternary systems is shown in Figure 7.

**3.7. Anisotropy Decay of TC in the Complexes of TC with Proteins.** In order to confirm the solvent exposed nature of the binding site of TC in the different proteins, we carried out anisotropy decay of TC in all the systems (Figure 8) with  $\lambda_{\text{exc}} = 370$  nm. The rotational correlation times ( $\theta_c$ ) recovered in the three systems are given in Table 2.

## 4. DISCUSSION

The ET process of the antenna effect in various rare earth ions [Ln(III)] from ligand donor usually takes place from the lowest triplet state ( $T_1$ ) of the donor following Dexter's exchange mechanism. We are not able to observe any  $T_1$  emission from TC in the free state or in any of the complexes at room temperature. However, we reported the location of the  $T_1$  state of TC at 77 K in our previous work.<sup>43,44</sup> The presence of a rise time of a few microseconds (Table 4) confirms the participation of the  $T_1$  state of TC in the sensitization process in the present systems.<sup>42,79–81</sup>

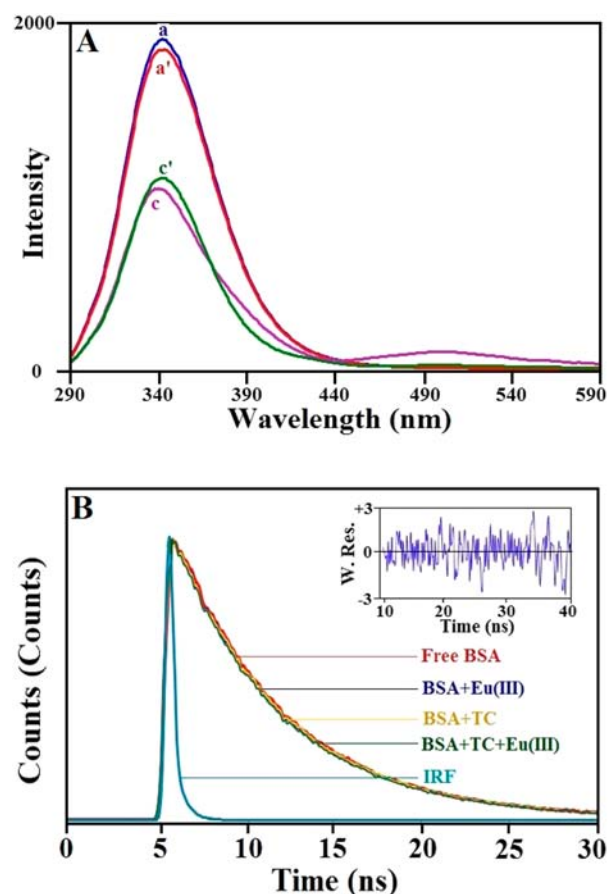


**Figure 4.** (A) Steady state fluorescence spectra of (a) BSA, (a') BSA + Eu(III), (c) BSA + TC, and (c') BSA + TC + Eu(III) in aqueous Tris-HCl buffer at pH 7.2 at 298 K.  $\lambda_{\text{exc}} = 280$  nm, excitation band pass = 10 nm, and emission band pass = 5 nm. [BSA] = 25  $\mu\text{M}$ , [TC] = 25  $\mu\text{M}$ , [Eu(III)] = 75  $\mu\text{M}$ . (B) Fluorescence decay of BSA in the pure state and in the different complexes in aqueous buffer at 298 K;  $\lambda_{\text{exc}} = 280$  nm,  $\lambda_{\text{monitor}} = 340$  nm (excitation band pass = 10 nm, emission band pass = 5 nm); [BSA] = 25  $\mu\text{M}$ , [TC] = 25  $\mu\text{M}$ , [Eu(III)] = 75  $\mu\text{M}$ .

**Table 3. Singlet State Lifetime of BSA, HSA, and AP (Monitoring Trp Emission) at 298 K in the Free State and in the Different Systems in Aqueous Buffer;  $\lambda_{\text{exc}} = 280$  nm**

system	$\tau_1$ (ns)	$\tau_2$ (ns)	$\langle \tau \rangle$ (ns)	$\chi^2$
free BSA	6.9 (66%)	4.8 (34%)	6.19	0.98
BSA + Eu(III)	7.0 (64%)	4.8 (36%)	6.20	1.02
BSA + TC	7.0 (62%)	4.7 (38%)	6.13	0.99
BSA + TC + Eu(III)	6.8 (71%)	4.0 (29%)	5.99	0.99
Free HSA	6.6 (51%)	2.8 (49%)	4.74	1.10
HSA + Eu(III)	6.6 (52%)	2.7 (48%)	4.73	0.98
HSA + TC	6.7 (47%)	2.8 (53%)	4.63	1.13
HSA + TC + Eu(III)	6.6 (46%)	2.8 (54%)	4.55	1.01
Free AP	4.9 (64%)	2.4 (36%)	4.00	0.91
AP + Eu(III)	4.8 (65%)	2.4 (35%)	3.96	1.08
AP + TC	4.7 (60%)	2.3 (40%)	3.74	1.06
AP + TC + Eu(III)	4.6 (58%)	2.3 (42%)	3.63	0.97

**4.1. Calculation of Energy Transfer (ET) Efficiency/Sensitization Efficiency and Radiative Lifetime of Eu(III).** The efficiency of ET was calculated using the equation<sup>42</sup>

$$\text{ET efficiency} = (A_{\text{acc}}/A_{\text{don}})[I_{\text{M}}/I_{\text{M}}^0 \times q_{\text{M}}^0/q_{\text{M}} - 1] \quad (6)$$

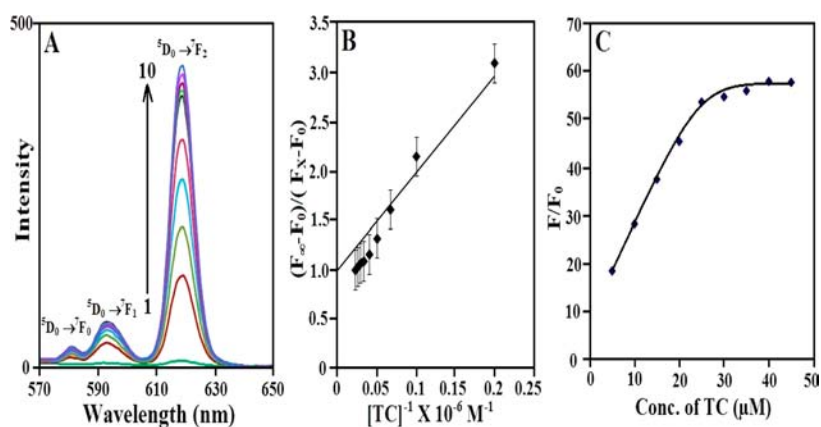


**Figure 5.** (A) Luminescence spectra of Eu(III) with varying concentrations of TC: (1) 0  $\mu\text{M}$ , (2) 5  $\mu\text{M}$ , (3) 10  $\mu\text{M}$ , (4) 15  $\mu\text{M}$ , (5) 20  $\mu\text{M}$ , (6) 25  $\mu\text{M}$ , (7) 30  $\mu\text{M}$ , (8) 35  $\mu\text{M}$ , (9) 40  $\mu\text{M}$ , and (10) 45  $\mu\text{M}$ , respectively, in aqueous buffer at 298 K, and in each case concentration of Eu(III) is kept at 75  $\mu\text{M}$ ;  $\lambda_{\text{exc}} = 395 \text{ nm}$ . Excitation band pass = 10 nm and emission band pass = 5 nm. (B) The plot of  $[F_{\infty} - F_0]/[F_x - F_0]$  vs  $[\text{TC}]$  obtained from modified Benesi-Hilderbrand equation at 298 K monitoring the peak at 618 nm of Eu(III) emission. (C) Plot of  $F/F_0$  against  $[\text{TC}]$ .

**Table 4. Luminescence Lifetime of Eu(III) [Monitored at 618 nm] at 298 K in Different Systems in Tris-HCl Buffer;  $\lambda_{\text{exc}} = 395 \text{ nm}$**

system	aqueous buffer						D <sub>2</sub> O buffer						
	$\tau_1$ ( $\mu\text{s}$ )	$\tau_2$ ( $\mu\text{s}$ )	$\tau_3$ ( $\mu\text{s}$ )	$\langle\tau\rangle^a$ ( $\mu\text{s}$ )	rise time ( $\mu\text{s}$ )	$\chi^2$	$\tau_1$ ( $\mu\text{s}$ )	$\tau_2$ ( $\mu\text{s}$ )	$\tau_3$ ( $\mu\text{s}$ )	$\langle\tau\rangle^a$ ( $\mu\text{s}$ )	rise time ( $\mu\text{s}$ )	$\chi^2$	$q^b$
free Eu(III) [Eu(NO <sub>3</sub> ) <sub>3</sub> ] at pH 7.2	140			140		1.10	332			332		1.20	
TC + Eu(III) at pH 7.2	104 (7%)	30 (93%)		35	4.2	1.05	143 (25%)	28 (75%)		57	4.2	1.15	11.8
BSA + TC + Eu(III) at pH 7.2	304 (7%)	143 (46%)	60 (47%)	115	7.4	1.20	641 (5%)	241 (30%)	89 (65%)	162	7.2	1.02	2.4
HSA + TC + Eu(III) at pH 7.2	299 (5%)	138 (41%)	63 (54%)	106	7.8	1.09	512 (9%)	172 (39%)	61 (52%)	145	7.6	1.10	2.5
AP + TC + Eu(III) at pH 8.0	180 (7%)	76 (31%)	23 (62%)	50	4.6	0.98	287 (8%)	84 (53%)	22 (39%)	80	4.7	0.97	7.9

<sup>a</sup>error in the analysis of  $\tau = \pm 5 \mu\text{s}$ . <sup>b</sup> $q$  is the number of coordinated water molecules calculated using the eq 12 considering the lifetime of ( $^5\text{D}_0 \rightarrow ^7\text{F}_2$  transition) band.

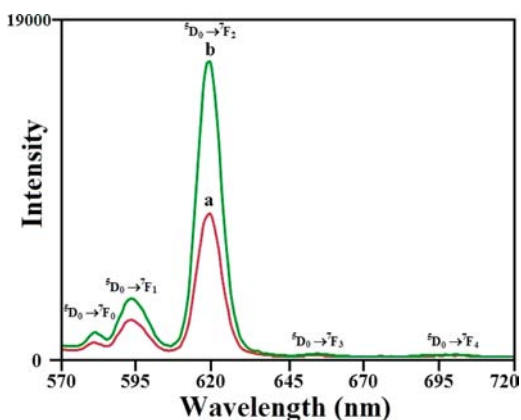


**Figure 6.** Luminescence spectra of Eu(III) in the ternary system consisting of BSA + TC + Eu(III) (a) in aqueous buffer and (b) in D<sub>2</sub>O buffer at 298 K;  $\lambda_{\text{exc}} = 395 \text{ nm}$ . Excitation band pass = 10 nm and emission band pass = 5 nm; [BSA] = 25  $\mu\text{M}$ , [TC] = 25  $\mu\text{M}$ , [Eu(III)] = 75  $\mu\text{M}$ .

where  $A_{\text{acc}}$  and  $A_{\text{don}}$  are the absorbances of the acceptor (Eu(III)) and donor, respectively, at the same excitation wavelength.  $I_{\text{M}}$  and  $I_{\text{M}}^0$  are the luminescence intensities of the Eu(III) in the presence and in the absence of energy transfer.  $q_{\text{M}}$  and  $q_{\text{M}}^0$  are the quantum yields of the Tb(III) in the

presence and in the absence of energy transfer, respectively. The factor  $q_{\text{M}}^0/q_{\text{M}}$  could be replaced by  $\tau_{\text{M}}^0/\tau_{\text{M}}$  assuming that  $k_{\text{r}}$  is relatively stable in all the systems, where  $\tau_{\text{M}}$  and  $\tau_{\text{M}}^0$  are the lifetimes in the presence and in the absence of energy transfer. The calculation of the ET efficiency ratio using the eq 6 includes the effect of both the shielding factor and the ET effect.

The ET efficiency ratios calculated for the  $^5\text{D}_0 \rightarrow ^7\text{F}_2$  peak at 618 nm of Eu(III) in the ternary systems compared to that in the binary systems are recorded in Table 5. The ET efficiency ratio ( $E_{\text{T}}/E_{\text{B}}$ ) of the ternary system for the transition  $^5\text{D}_0 \rightarrow ^7\text{F}_2$  when compared to that of the binary complex of TC and Eu(III) is very significant for HSA and BSA (18.3 for BSA and 18.7 for HSA), the ratio ( $E_{\text{T}}/E_{\text{B}}$ ) for the ternary system of AP and TC with Eu(III), however, is not so significant, and it is only 1.7 in aqueous buffer (Table 5).

One could also visualize the sensitization efficiency ( $\eta_{\text{sens}}$ ) of the complex upon excitation of the ligand, TC, using the equation<sup>82</sup>

$$\phi_{\text{tot}} = \eta_{\text{sens}} \phi_{\text{Ln}} \quad (7)$$

where  $\phi_{\text{tot}}$  is the overall luminescence quantum yield and  $\phi_{\text{Ln}}$  the quantum yield of the lanthanide luminescence step.  $\phi_{\text{tot}}$  can be readily measured from the steady state emission spectra. The overall luminescence quantum yield ( $\phi_{\text{tot}}$ ) of the complex is calculated using the equation<sup>82</sup>

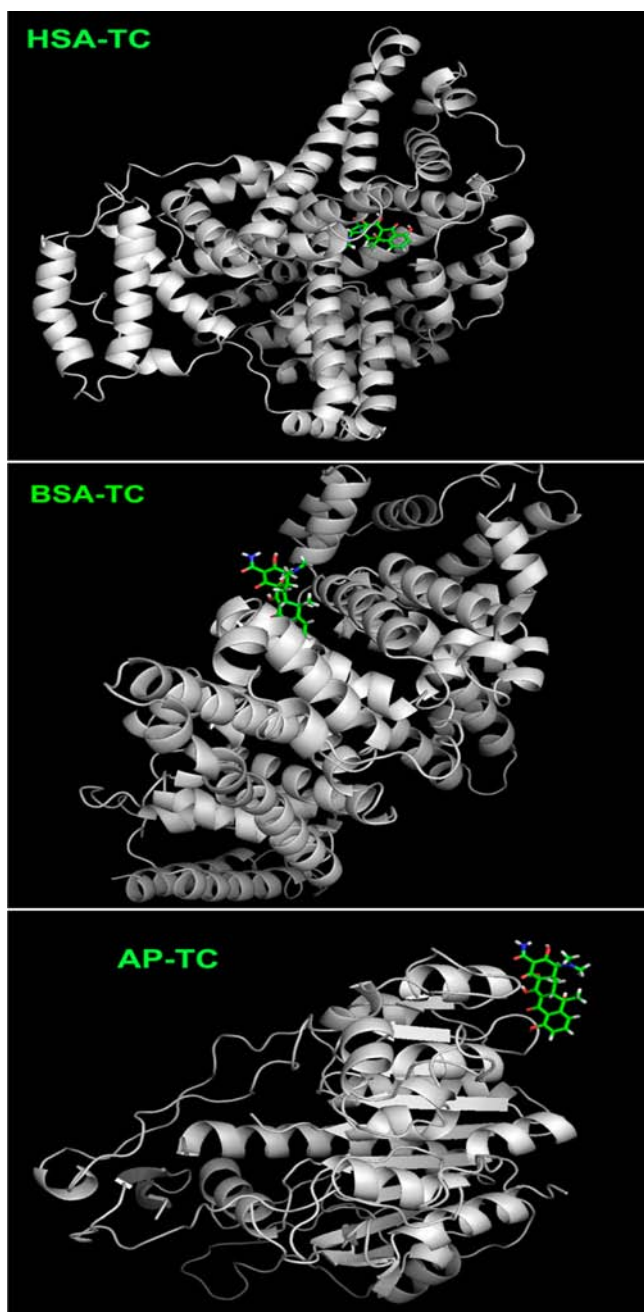


Figure 7. Docked pose of TC in different proteins.

$$(\phi_{\text{tot}})_{\text{u}} / (\phi_{\text{tot}})_{\text{ref}} = n_{\text{u}}^2 I_{\text{u}} A_{\text{ref}} / n_{\text{ref}}^2 I_{\text{ref}} A_{\text{u}} \quad (8)$$

where  $n_{\text{u}}$ ,  $I_{\text{u}}$ , and  $A_{\text{u}}$  are the refractive index, the area of the corrected emission spectrum, and the absorbance at the excitation wavelength, respectively, for the measuring complex.  $n_{\text{ref}}$ ,  $I_{\text{ref}}$ , and  $A_{\text{ref}}$  are the same observables for the reference sample.

If the radiative lifetime,  $\tau_{\text{R}}$ , is known,  $\phi_{\text{Ln}}$  can be calculated from the observed luminescence lifetime ( $\tau_{\text{obs}}$ ) using the following equation

$$\phi_{\text{Ln}} = k_{\text{r}} / (k_{\text{r}} + k_{\text{nr}}) = \tau_{\text{obs}} / \tau_{\text{R}} \quad (9)$$

where  $k_{\text{r}}$  and  $k_{\text{nr}}$  are the rate constants of radiative and nonradiative deactivation.

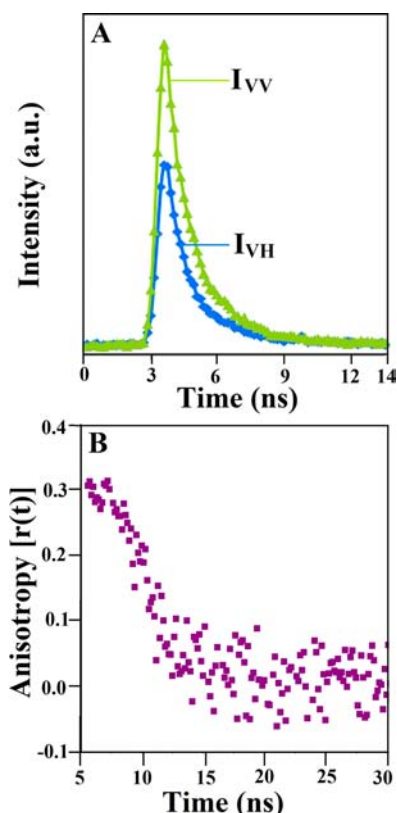


Figure 8. (A)  $I_{\text{VV}}$  and  $I_{\text{VH}}$  represent decays of the emission band at 498 nm of TC in BSA–TC complex with excitation polarizer at the vertical position and emission polarizer at the vertical and horizontal positions, respectively.  $\lambda_{\text{exc}} = 370$  nm; excitation and emission band pass = 10 nm each; (B) fluorescence anisotropy decay of TC (25  $\mu\text{M}$ ) monitoring the emission band at 498 nm at 298 K in the BSA-TC complex.

In Eu(III), the transition from  ${}^5\text{D}_0 \rightarrow {}^7\text{F}_j$  ( $J = 0,3,5$ ) is magnetic dipole as well as induced electric dipole forbidden. The transition  ${}^5\text{D}_0 \rightarrow {}^7\text{F}_j$  ( $J = 2,4,6$ ) is purely of induced electric dipole nature.<sup>82</sup> Assuming that both the energy of the  ${}^5\text{D}_0 \rightarrow {}^7\text{F}_1$  transition (only magnetic dipole allowed without any electric dipole contribution) and its dipole strength are constant, Verhoeven et al. found that the radiative lifetime ( $\tau_{\text{R}}$ ) of the complex is given by the following equation<sup>82</sup>

$$1/\tau_{\text{R}} = A_{\text{MD},\text{O}} n^3 (I_{\text{tot}}/I_{\text{MD}}) \quad (10)$$

where  $n$  is the refractive index of the medium (solvent),  $A_{\text{MD},\text{O}}$  is the spontaneous emission probability for the magnetic dipole (MD) allowed  ${}^5\text{D}_0 \rightarrow {}^7\text{F}_1$  transition, and  $(I_{\text{tot}}/I_{\text{MD}})$  is the ratio of the total area of the corrected Eu(III) emission spectra to the area of the  ${}^5\text{D}_0 \rightarrow {}^7\text{F}_1$  band. Theoretical calculation showed that the value of  $A_{\text{MD},\text{O}}$  is  $14.65 \text{ s}^{-1}$ .<sup>82</sup> The radiative lifetime ( $\tau_{\text{R}}$ ) and the quantum yield of lanthanide emission ( $\phi_{\text{Ln}}$ ) of the Eu(III) ion are calculated in the different binary and in the ternary systems (Table 5). The overall quantum yield ratio ( $(\phi_{\text{tot}})_{\text{T}} / (\phi_{\text{tot}})_{\text{B}}$ ) and sensitization efficiency ratio ( $(\eta_{\text{sens}})_{\text{T}} / (\eta_{\text{sens}})_{\text{B}}$ ) of the different ternary systems compared to  $\text{Eu}_3\text{TC}$  are also calculated (Table 5). It is observed that the sensitization efficiency ratio ( $(\eta_{\text{sens}})_{\text{T}} / (\eta_{\text{sens}})_{\text{B}}$ ) of the ternary systems (6.8 for BSA and TC with Eu(III) and 6.9 for HSA and TC with Eu(III)) is very significant compared to the binary complex,  $\text{Eu}_3\text{TC}$ . However, it is quite low (= 1.34) for the ternary system of AP and TC with Eu(III) (Table 5).



**Table 5. Sensitization Efficiency ( $\eta_{\text{sens}}$ ) Ratio, Energy Transfer Efficiency ( $E$ ) Ratio, Radiative Lifetime ( $\tau_{\text{R}}$ ), and the Experimental Overall Luminescence Quantum Yield ( $\phi_{\text{tot}}$ ) Ratio of Eu(III) in the Different Systems Calculated on the Basis of the Observed Emission Spectra and Life Time Upon Ligand Excitation at 395 nm at 298 K<sup>a</sup>**

system	$\tau_{\text{R}}$ from eq 10	$\phi_{\text{Ln}}$ from eq 9	quantum yield ratio $[(\phi_{\text{tot}})_{\text{T}}/(\phi_{\text{tot}})_{\text{B}}]$ using eq 8	sensitization efficiency ratio $[(\eta_{\text{sens}})_{\text{T}}/(\eta_{\text{sens}})_{\text{B}}]$ using eq 7	$E_{\text{T}}/E_{\text{B}}$ at 618 nm ( ${}^5\text{D}_0 \rightarrow {}^7\text{F}_2$ transition) using eq 6
TC + Eu(III)	3.28 ms (3.27 ms)	0.010 (0.017)			
BSA + TC + Eu(III)	3.91 ms (3.90 ms)	0.029 (0.040)	17.9 (17.8)	6.8 (7.6)	5.5 (6.3)
HSA + TC + Eu(III)	4.02 ms (3.92 ms)	0.026 (0.037)	17.8 (17.8)	6.9 (8.2)	5.9 (7.2)
AP + TC + Eu(III)	3.52 ms (3.16 ms)	0.014 (0.025)	1.7 (2.4)	1.3 (1.6)	1.1 (1.7)

<sup>a</sup> $E_{\text{T}}$  = Energy transfer efficiency of ternary systems.  $E_{\text{B}}$  = Energy transfer efficiency of binary system of TC and Eu(III). Error in the energy transfer efficiency ratio =  $\pm 2\%$ . The results obtained in D<sub>2</sub>O are given in parentheses.

The ET efficiency ( $E$ ) ratio and the sensitization efficiency ( $\eta_{\text{sens}}$ ) ratio of the emission of Eu(III) in the ternary systems compared to Eu<sub>3</sub>TC in D<sub>2</sub>O buffer have also been calculated and are presented in Table 5.

**4.2. Mechanism of Antenna Effect.** **4.2.1. Determination of the Number of Coordinated "H<sub>2</sub>O".** The lifetime ( $\tau$ ) of Eu(III) can be expressed as<sup>83</sup>

$$1/\tau = k_{\text{r}} + k_{\text{nr}} + k_{\text{q}} \quad (11)$$

where  $k_{\text{r}}$ ,  $k_{\text{nr}}$ , and  $k_{\text{q}}$  are the rate constants of the radiative, the nonradiative, and the quenching deactivation (due to presence of any quencher or due to the microenvironment of Eu(III) in the systems), respectively. The rate constant  $k_{\text{nr}}$ <sup>84,85</sup> and  $k_{\text{q}}$  control the lifetime. In order to find the difference of the microenvironment of Eu(III), one can utilize the lifetime of Eu(III) in all the complexes in H<sub>2</sub>O and D<sub>2</sub>O. The numbers of coordinated "H<sub>2</sub>O" in all the binary and the ternary systems using the equation developed by Horrocks and Supkowski<sup>86,87</sup> are given in Table 4. The number of H<sub>2</sub>O molecules coordinated ( $q$ ) in the inner sphere of the complex is given by

$$q = 1.1[\tau_{\text{H}_2\text{O}}^{-1} - \tau_{\text{D}_2\text{O}}^{-1} - 0.31] \quad (12)$$

where  $\tau_{\text{H}_2\text{O}}$  and  $\tau_{\text{D}_2\text{O}}$  are the lifetimes in ms of Eu(III) in various complexes in H<sub>2</sub>O and D<sub>2</sub>O buffer, respectively. The value of  $q$  decreases from 11.6 in the Eu<sub>3</sub>TC to 2.5 in the ternary system of HSA/BSA whereas the value of  $q$  is 8 in the ternary system of AP (Table 4). The drastic decrease of  $q$  values calculated thus clearly demonstrates that Eu(III) is very well shielded from "H<sub>2</sub>O" in the ternary complexes containing HSA/BSA compared to that in the binary complexes. This shielding effect which reduces the vibronic coupling with O–H oscillator could decrease the quenching rate ( $k_{\text{nr}}$  and  $k_{\text{q}}$ ) of Eu(III) in the ternary complexes leading to enhanced emission of Eu(III). The results obtained for the AP system imply that the decrease in  $q$  is not enough to enhance the sensitization efficiency significantly.

**4.2.2. Docking Studies Locating the Binding Site of TC.** The docked pose clearly indicates that TC binds on the surface of AP whereas the binding site is within the interior of the proteins HSA and BSA (Figure 7, Table 2). This is reflected in the total loss of ASA of different residues of the proteins involved in the binding (Table 2). It is also interesting to note that the ASA values of the ligand TC are different in the different systems (Table 2). The large value of ASA of TC in the case of AP is further indication of solvent exposed nature of TC in the complex with AP. Figure 9 and Table 6 depict the various residues of proteins which are in close proximity

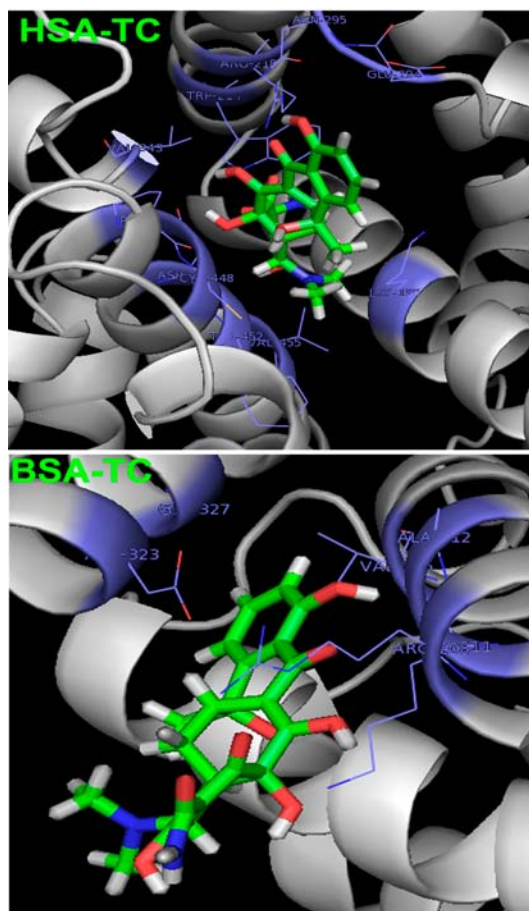


**Figure 9.** Various residues present within 4 Å of the probe, TC, in the serum albumins.

(within 4 Å) with various functional groups in TC. From Table 6 it is seen that the number of neighboring atoms of the different residues within 4 Å from the different functional groups of bound TC is more in the HSA-TC and BSA-TC complexes compared to that in the AP-TC complex.

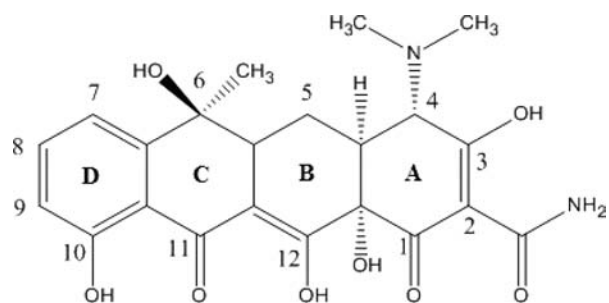
**4.2.3. Anisotropy Decay of TC in the Complexes.** The value of rotational correlation time ( $\theta_{\text{C}}$ ) obtained from the anisotropy decay reflects the motional restriction of a probe. The data in Table 2 show that the rotation of TC is much faster in the AP-TC complex compared to that in HSA-TC or BSA-TC complexes. The results clearly indicate that TC experiences more freedom in the AP-TC complex, confirming the large solvent accessibility of TC.

Table 6. Different Atoms of Different Residues of Serum Albumins and AP within 4 Å from the Different Binding Sites of TC

TC <sup>a</sup>	HSA <sup>b</sup>	BSA <sup>b</sup>	AP <sup>b</sup>
O of 1-C=O	Arg 218 (CD[3.4], NH1[3.1])	Arg 208 (CG[3.7], CD[3.8], NE[2.8], CZ[3.5], NH1[3.4])	Trp 220 (CE2[3.5], NE1[2.7], CD1[4.0]), Ala 231 (C[4.0], O[3.5])
O of 2-CONH <sub>2</sub>	Trp 214 (NE1[3.2], CZ2[3.6], CE2[3.7])	Arg 208 (NH1[3.0])	Trp 220 (CD1[3.6], NE1[3.1]), Ala 231 (CB[3.6]), Lys 223 (NZ[3.2])
N of 2-CONH <sub>2</sub>	Trp 214 (NE1[3.7], CE2[3.5], CZ2[2.5], CH2[3.5])		
O of 3-COH	Val 455 (CG2[3.5]), Tyr 452 (N[3.8]), Asp 451 (C[3.4], O[3.1], CB[3.5])		
N of 4-CN(Me) <sub>2</sub>			
O of 6-COH	Cys 448 (CA[3.7])		
O of 10-COH	Asn 295 (ND2[2.5], CG[3.0], OD1[3.0], N[4.0])	Arg 208 (O[2.9], C[3.7], CA[4.0]), Ala 212 (N[3.6], CA[4.0])	
O of 11-C=O	Arg 218 (NH1[2.5], CZ[3.3], NH2[3.3]), Asn 295 (ND2[3.8])	Arg 208 (O[3.5], C[3.6], CA[2.7], CB[2.8], CG[2.8], CD[3.9], N[3.9]), Lys 211 (CB[4.0])	Arg 232 (CG[3.3], CD[3.8], CB[3.4], NE[3.1])
O of 12-COH group of B ring	Arg 218 (CZ[3.8], NH1[2.5]), Pro 447 (CB[3.5]), Asp451 (OD2[3.9])	Arg 208 (CA[3.4], CB[3.5], CG[2.6], CD[3.8], NE[3.9], N[3.6]), Lys 211 (NZ[3.3], CD[3.7], CE[3.5])	Ala231 (O[2.9], C[3.6]), Arg 232 (O[3.8], C[3.5], CA[2.7], N[3.5])
O of 1-C-C(OH)-C-12	Pro 447 (CA[3.8]), Asp 451 (OD2[2.6], CG[3.0], CB[3.7]), Cys 448 (N[3.9])	Lys 211 (NZ[2.5], CE[3.7])	

<sup>a</sup>See Scheme 1 for the numbering of functional groups of TC. <sup>b</sup>Values within [] indicate the closest distance in Å. Atom name according to PYMOL.<sup>72</sup>

Scheme 1. Structure of Tetracycline (TC)



Thus, docking results and  $\theta_c$  values clearly confirm that Eu(III) is more susceptible to couple with the O–H oscillator in the ternary system containing AP whereas Eu(III) is well shielded in the ternary system containing HSA and BSA.

The quantum yield ( $\phi$ ) of bound TC in AP is greater than that in HSA/BSA (Table 2). This is in conformity with the larger binding constant (Table 2) and enhanced ET from the Trp 109 residue in AP which lies very near to TC.<sup>43</sup> One could thus expect that ET from TC to Eu(III) in the ternary system containing AP should be efficient. However, the quenching of TC emission in the ternary system of AP with TC and Eu(III) is observed to be much less. The results probably imply that the donor moiety of TC is unfavorably situated with respect to Eu(III), diminishing ET efficiency assuming that Dexter's exchange mechanism is operative. However, the results of efficient quenching of TC emission in the system of HSA/BSA with TC and Eu(III) clearly indicate enhanced ET from TC to Eu(III). The lowest triplet state ( $T_1$ ) of free TC has been found to be  $19500\text{ cm}^{-1}$ .<sup>43</sup> The energy gap between the  $T_1$  and  $^5D_0$  of Eu(III) is  $\approx 2250\text{ C m}^{-1}$ , a value which could minimize the back ET from Eu(III)

## 5. CONCLUSION

(i) A ternary system consisting a protein (HSA/BSA), TC, and Eu(III) has been developed and shown to exhibit highly efficient "antenna effect" compared to Eu<sub>3</sub>TC complex. The sensitization effect is found to be greater than that in the

Eu<sub>3</sub>TC–H<sub>2</sub>O<sub>2</sub> system. The donor in each case is observed to be TC since the enhanced emission of TC in the binary complex containing HSA/BSA and TC almost gets completely quenched in the ternary systems.

(ii) However, the enhancement of Eu(III) emission in the ternary system containing AP, TC, and Eu(III) is not significant compared to that of the Eu<sub>3</sub>TC complex. This is in contrast to the observed binding constant of the complex of TC with AP (the binding constant being 2 orders of magnitude greater than the complex of TC with HSA/BSA) and the quantum yield ( $\phi$ ) of TC in the AP–TC complex ( $\phi$  being much greater than that in the complex of TC with HSA/BSA).

(iii) The almost total quenching of the TC emission observed in the ternary system HSA/BSA, TC, and Eu(III) clearly shows an efficient energy transfer (ET) from TC to Eu(III) in these systems.

(iv) The energy transfer efficiency ratio ( $E_T/E_B$ ), the sensitization efficiency ratio [ $(\eta_{\text{sen}})_T/(\eta_{\text{sen}})_B$ ], and the radiative lifetime of Eu(III) have been calculated in all the ternary systems using the steady state and time-resolved measurement of Eu(III) emission showing the large "antenna effect" in the systems containing serum albumins (HSA/BSA).

(v) The highly efficient "antenna effect" observed in the system containing HSA/BSA has been explained due to the binding of Eu<sub>3</sub>TC in the interior of the protein. This is evidenced by the determination of  $q$  (the number of coordinated H<sub>2</sub>O in the primary sphere of Eu(III)) from time-resolved data in H<sub>2</sub>O and D<sub>2</sub>O.

(vi) Docking studies clearly show that TC binds to the surface of the protein in the AP–TC complex, whereas TC binds in the hydrophobic interior region in the case of the complex with HSA/BSA. The location of the binding site in the case of HSA/BSA prevents vibronic coupling with the O–H oscillator.

(vii) The rotational correlation time of bound TC and ASA of TC in all the systems also support the shielding of Eu(III) in the complex of HSA/BSA and the solvent exposed nature of TC in the AP–TC complex.

(viii) The lowest triplet state energy of TC is found to be favorable for efficient ET from TC to Eu(III); the energy gap

between the triplet of TC and the  $^5D_1$  or  $^5D_0$  level of Eu(III) minimizes the back ET.

## AUTHOR INFORMATION

### Corresponding Author

\*Tel.: +9133-22413893, +919836940620. E-mail: sanjibg@cal2.vsnl.net.in, pchemsg@gmail.com.

### Notes

The authors declare no competing financial interest.

## ACKNOWLEDGMENTS

S.G. gratefully acknowledges DST (SR/S1/PC-57/2008) and CSIR (No. 21(0871)/11/EMR-II) for financially supporting this work. S.K.G. acknowledges CSIR for SRF fellowship (No.08/155(0038)/2009-EMR-I), and S.K.S. thanks CSIR for the SRF fellowship (No.08/155(0039)/2009-EMR-I), respectively. M.M. and P.S.S. thanks DST for the SRF and RA fellowships, respectively (No.SR/S1/PC-57/2008).

## REFERENCES

- Oshishi, Y.; Kanamori, T.; Kitagawa, Y.; Takashashi, S.; Snitzer, E.; Sigel, G. H., Jr. *Opt. Lett.* **1991**, *16*, 1747–1749.
- Mears, R. J.; Baker, S. R. *Opt. Quantum Electron.* **1992**, *24*, 517–538.
- Desurvire, E. *Phys. Today* **1994**, *47*, 20–27.
- Piguet, C.; Bünzli, J.-C. G. *Chem. Soc. Rev.* **1999**, *28*, 347–358.
- Merbach, A. E.; Toth, E., Eds. *The Chemistry of Contrast Agents in Medical Magnetic Resonance Imaging*; John Wiley: London, 2001.
- Cui, Y.; Yue, Y.; Qian, G.; Chen, B. *Chem. Rev.* **2012**, *112* (2), 1126–1162.
- Cotton, S. *Lanthanide and Actinide Chemistry*; Wiley, New York, 2006.
- de Sá, G. F.; Malta, O. L.; De Mello Donegá, C.; Simas, A. M.; Longo, R. L.; Santa-Cruz, P. A.; da Silva, E. F., Jr. *Coord. Chem. Rev.* **2000**, *196*, 165–195.
- Yang, X.; Jones, R. A. *J. Am. Chem. Soc.* **2005**, *127*, 7686–7687.
- Pan, N.; Bian, Y.; Fukuda, T.; Yokoyama, M.; Li, R.; Neya, S.; Jiang, J.; Kobayashi, N. *Inorg. Chem.* **2004**, *43*, 8242–8244.
- Fratini, A.; Richards, G.; Larder, E.; Swavey, S. *Inorg. Chem.* **2008**, *47*, 1030–1036.
- Yan, B.; Li, Y.-Y.; Guo, L. *Inorg. Chem. Commun.* **2011**, *14*, 910–912.
- Horrocks, W. D.; Sudnick, D. R. *Acc. Chem. Res.* **1981**, *14*, 384–392.
- Bünzli, J.-C. G.; Piguet, C. *Chem. Rev.* **2002**, *102*, 1897–1928.
- Pope, S. J. A.; Coe, B. J.; Faulkner, S.; Bichenkova, E. V.; Yu, X.; Douglas, K. T. *J. Am. Chem. Soc.* **2004**, *126*, 9490–9491.
- Shavaleev, N. M.; Moorcraft, L. P.; Pope, S. J. A.; Bell, Z. R.; Faulkner, S.; Ward, M. D. *Chem. Commun.* **2003**, *10*, 1134–1135.
- Torelli, S.; Imbert, D.; Cantuel, M.; Bernardinelli, G.; Delahaye, S.; Hauser, A.; Bünzli, J.-C. G.; Piguet, C. *Chem.-Eur. J.* **2005**, *11*, 3228–3242.
- Shavaleev, N. M.; Moorcraft, L. P.; Pope, S. J. A.; Bell, Z. R.; Faulkner, S.; Ward, M. D. *Chem.-Eur. J.* **2003**, *9*, 5283–5291.
- Sun, Y.-Q.; Zhang, J.; Yang, G.-Y. *Chem. Commun.* **2006**, *45*, 4700–4702.
- Faulkner, S.; Matthews, J. L. In *Comprehensive Coordination Chemistry, Application of Coordination of Complexes*, 2nd ed.; Ward, M. D., Ed.; Elsevier: Oxford, U.K., 2004; pp 913–944.
- Brunet, E.; Juanes, O.; Rodriguez-Ubis, J. C. *Curr. Chem. Biol.* **2007**, *1*, 11–39.
- Picot, A.; D'Aleo, A.; Baldeck, P. L.; Grichine, A.; Duperray, A.; Andraud, C.; Maury, O. *J. Am. Chem. Soc.* **2008**, *130*, 1532–1533.
- Kielar, F.; Congreve, A.; Law, G.-L.; New, E. J.; Parker, D.; Wong, K.; Castreo, P.; de Mendoza, J. *Chem. Commun.* **2008**, 2435–2437.
- Palsson, L. O.; Pal, R.; Murray, B. S.; Parker, D.; Beeby, A. *Dalton Trans.* **2007**, 5726–5734.
- Werts, M. H. V.; Nerambourg, N.; Pelegry, D.; Grand, Y. L.; Blanchard-Desce, M. *Photochem. Photobiol. Sci.* **2005**, *4*, 531–538.
- Bünzli, J.-C. G. In *Metal Ions in Biological Systems*; Sigel, A., Ed.; Marcel Dekker Inc.: New York, 2004; Vol. 42, Ch 2.
- Binnemans, K. *Chem. Rev.* **2009**, *109*, 4283–4374.
- Nonat, A. M.; Allain, C.; Faulkner, S.; Gunnlaugsson, T. *Inorg. Chem.* **2010**, *49*, 8449–8456.
- Li, S.-M.; Zheng, X.-J.; Yuan, D.-Q.; Ablet, A.; Jin, L.-P. *Inorg. Chem.* **2012**, *51*, 1201–1203.
- Dehaen, G.; Verwilt, P.; Eliseeva, S. V.; Laurent, S.; Elst, L. V.; Muller, R. N.; De Borggraeve, W. M.; Binnemans, K.; Parac-Vogt, T. N. *Inorg. Chem.* **2011**, *50*, 10005–10014.
- Xu, H.-B.; Chen, Z.-N. *Inorg. Chem. Commun.* **2011**, *14*, 1609–1611.
- Shinoda, S.; Mizote, A.; Masaki, M. E.; Yoneda, M.; Miyake, H.; Tsukube, H. *Inorg. Chem.* **2011**, *50*, 5876–5878.
- Sykes, D.; Tidmarsh, I. S.; Barbieri, A.; Sazanovich, I. V.; Weinstein, J. A.; Ward, M. D. *Inorg. Chem.* **2011**, *50*, 11323–11339.
- Pope, S. J. A.; Coe, B. J.; Faulkner, S.; Bichenkova, E. V.; Yu, X.; Douglas, K. T. *J. Am. Chem. Soc.* **2004**, *126*, 9490–9491.
- Lazarides, T.; Tart, N. M.; Sykes, D.; Faulkner, S.; Barbieri, A.; Ward, M. D. *Dalton Trans.* **2009**, 3971–3979.
- Koullourou, T.; Natrajan, L. S.; Bhavsar, H.; Pope, S. J. A.; Feng, J.; Narvainen, J.; Shaw, R.; Scales, E.; Kauppinen, R.; Kenwright, A. M.; Faulkner, S. *J. Am. Chem. Soc.* **2008**, *130*, 2178–2179.
- Jiang, W.; Lou, B.; Wang, J.; Lv, H.; Bian, Z.; Huang, C. *Dalton Trans.* **2011**, *40*, 11410–11418.
- Herrera, J.-M.; Pope, S. J. A.; Adams, H.; Faulkner, S.; Ward, M. D. *Inorg. Chem.* **2006**, *45*, 3895–3904.
- Lazarides, T.; Sykes, D.; Faulkner, S.; Barbieri, A.; Ward, M. D. *Chem.—Eur. J.* **2008**, *14*, 9389–9399.
- Senechal-David, K.; Pope, S. J. A.; Quinn, S.; Faulkner, S.; Gunnlaugsson, T. *Inorg. Chem.* **2006**, *45*, 10040–10042.
- Davies, G. M.; Pope, S. J. A.; Adams, H.; Faulkner, S.; Ward, M. D. *Inorg. Chem.* **2005**, *44*, 4656–4665.
- Ghorai, S. K.; Samanta, S. K.; Mukherjee, M.; Ghosh, S. *J. Phys. Chem. A* **2012**, *116*, 8303–8312.
- Mukherjee, M.; Saha Sardar, P.; Ghorai, S. K.; Samanta, S. K.; Singha Roy, A.; Dasgupta, S.; Ghosh, S. *J. Photochem. Photobiol., B* **2012**, *115*, 93–104.
- Ghosh, S. Unpublished Results.
- Courrol, L. C.; Samad, R. E. *Curr. Pharm. Anal.* **2008**, *4*, 238–248.
- Courrol, L. C.; Silva, F. R.; de, O.; Gomes, L.; Júnior, N. D. V. *J. Lumin.* **2007**, *122*, 288–290.
- Hirsch, L. M.; Van Geel, T. F.; Winefordner, J. D.; Kelly, R. N.; Schulman, S. G. *Anal. Chim. Acta* **1984**, *166*, 207–219.
- Celotti, M.; Fazakerley, G. V. *J. Chem. Soc., Perkin Trans. 2* **1977**, *2*, 1319–1322.
- Moriyama, Y.; Ohta, D.; Hachiya, K.; Mitsui, Y.; Takeda, K. *J. Protein Chem.* **1996**, *15*, 265–272.
- He, X. M.; Carter, D. C. *Nature* **1992**, *358*, 209–215.
- Brown, J. R. *Proc. FEBS Meet.* **1977**, *50*, 1–20.
- Brown, J. R. In *Albumin: Structure, Function, and Uses*; Rosenoer, V. M., Oratz, M., Rothschild, M. A., Eds.; Pergamon Press: Oxford, 1977; pp 27–51.
- Bosron, W. F.; Anderson, R. A.; Falk, M. C.; Kennedy, F. S.; Vallee, B. L. *Biochemistry* **1977**, *16*, 610–614.
- Philipps, D. A. *Metals and Metabolism*; Oxford University Press: 1976; p 63.
- Young, A. D.; Noble, R. W. *Methods Enzymol.* **1981**, *76*, 792–793.
- Bowler, B. E.; Lippard, S. J. Ph.D. Dissertation. Massachusetts Institute of Technology, 1987.
- Malinge, J. M.; Schwartz, A.; Leng, M. *Nucleic Acid Res.* **1987**, *15*, 1779–1797.

- (58) Hough, E.; Hansen, L. K.; Birknes, B.; Jynge, K.; Hansen, S.; Hordvik, A.; Little, C.; Dodson, E. J.; Derewenda, Z. *Nature* **1989**, *338*, 357–360.
- (59) Volbeda, A.; Lahm, A.; Sakiyama, F.; Suck, D. *EMBO J.* **1991**, *10*, 1607–1618.
- (60) Anderson, R. A.; Borson, W. F.; Kennedy, F. S.; Vallee, B. L. *Proc. Natl. Acad. Sci. U.S.A.* **1975**, *72*, 2989–2993.
- (61) Tibbitts, T. T.; Murphy, J. E.; Kantrowitz, E. R. *J. Mol. Biol.* **1996**, *257*, 700–715.
- (62) Stec, B.; Holtz, K. M.; Kantrowitz, E. R. *J. Mol. Biol.* **2000**, *299*, 1303–1311.
- (63) Demas, J. N.; Crosby, G. A. *J. Phys. Chem.* **1971**, *75*, 991–1024.
- (64) Bevington, P. R. *Data Reduction and Error Analysis for the Physical Sciences*; McGraw Hill: New York, 1969; pp 235–237.
- (65) *FELIX 32*, Operation Manual, Version 1.1; Photon Technology International, Inc.: NJ, 2003.
- (66) Berman, H. M.; Westbrook, J.; Feng, Z.; Gilliland, G.; Bhat, T. N.; Weissig, H.; Shindyalov, I. N.; Bourne, P. E. *Nucleic Acids Res.* **2000**, *28*, 235–242.
- (67) Karplus, K.; Katzman, S.; Shackelford, G.; Koeva, M.; Draper, J.; Barnes, B.; Soriano, M.; Hughey, R. *Proteins: Struct., Funct. Bioinform.* **2005**, *61* (S7), 135–142.
- (68) Karchin, R.; Cline, M.; Karplus, K. *Proteins: Struct., Funct. Genet.* **2004**, *55*, 508–518.
- (69) Karchin, R.; Cline, M.; Mandel-Gutfreund, Y.; Karplus, K. *Proteins: Struct., Funct. Genet.* **2003**, *51*, 504–514.
- (70) Karplus, K.; Karchin, R.; Draper, J.; Casper, J.; Mandel-Gutfreund, Y.; Diekhans, M.; Hughey, R. *Proteins: Struct., Funct. Genet.* **2003**, *53* (S6), 491–496.
- (71) Karplus, K.; Karchin, R.; Barrett, C.; Tu, S.; Cline, M.; Diekhans, M.; Grate, L.; Casper, J.; Hughey, R. *Proteins: Struct., Funct. Genet.* **2001**, *45*, 86–91.
- (72) De Lano, W. L. *The PyMOL molecular graphics system*; San Carlos, CA: DeLano Scientific; 2004. <http://www.pymol.sourceforge.net>.
- (73) Sytnik, A.; Litvinyuk, I. *Proc. Natl. Acad. Sci. U.S.A.* **1996**, *93*, 12959–12963.
- (74) Beechem, J. M.; Brand, L. *Annu. Rev. Biochem.* **1985**, *54*, 43–71.
- (75) Benesi, A. H.; Hilderbrand, J. H. *J. Am. Chem. Soc.* **1949**, *71*, 2703–2707.
- (76) Maity, S. S.; Samanta, S.; Saha Sardar, P.; Pal, A.; Dasgupta, S.; Ghosh, S. *Chem. Phys.* **2008**, *354*, 162–173.
- (77) Pal, A.; Maity, S. S.; Samanta, S.; Saha Sardar, P.; Ghosh, S. *J. Lumin.* **2010**, *130*, 1975–1982.
- (78) Dehaen, G.; Absillis, G.; Driesen, K.; Binnemans, K.; Parac-Vogt, T. N. *Helv. Chim. Acta* **2009**, *92*, 2387–2397.
- (79) Schlyer, B. D.; Steel, D. G.; Gafni, A. *J. Biol. Chem.* **1995**, *270*, 22890–22894.
- (80) Ghosh, S.; Misra, A.; Ozarowski, A.; Maki, A. H. *J. Phys. Chem. B* **2003**, *107*, 11520–11526.
- (81) Samanta, S. K.; Ghorai, S. K.; Ghosh, S. *J. Photochem. Photobiol., A* **2013**, *252*, 145–151.
- (82) Werts, M. H. V.; Jukes, R. T. F.; Verhoeven, J. W. *Phys. Chem. Chem. Phys.* **2002**, *4*, 1542–1548.
- (83) Brown, T. D.; Shepherd, T. M. *J. Chem. Soc.: Dalton Trans.* **1973**, *3*, 336–339.
- (84) Sun, C.; Yang, J.; Wu, X.; Su, B.; Liu, S. *Chem. Phys. Lett.* **2004**, *398*, 343–350.
- (85) Pal, A.; Maity, S. S.; Samanta, S.; Saha Sardar, P.; Ghosh, S. *J. Lumin.* **2010**, *130*, 1975–1982.
- (86) Supkowski, R. M.; Horrocks, W. D. *Inorg. Chim. Acta* **2002**, *340*, 44–48.
- (87) Faulkner, S.; Natrajan, L. S.; Perry, W. S.; Sykes, D. *Dalton Trans.* **2009**, *20*, 3890–3899.